The Cryosphere Discuss., https://doi.org/10.5194/tc-2017-192
Manuscript under review for journal The Cryosphere
Discussion started: 22 September 2017
© Author(s) 2017. CC BY 4.0 License.

The Cryosphere Discussions
Open Access
EGU

Atmospheric influences on the anomalous 2016 Antarctic sea ice decay

Elisabeth Schlosser[1,2], F. Alexander Haumann[3], Marilyn N. Raphael[4]

[1]Institute of Atmospheric and Cryospheric Sciences, University of Innsbruck, Innsbruck, Austria}

[2]Austrian Polar Research Institute, Vienna, Austria}

[3]Environmental Physics, Inst. of Biogeochemistry and Pollutant Dynamics , ETH Zürich, Zürich, Switzerland}

[4]Department of Geography, University of California, Los Angeles, California, USA}

Correspondence to: E. Schlosser (Elisabeth.Schlosser@uibk.ac.at)

Abstract In contrast to the Arctic, where total sea ice extent (SIE) has been decreasing for the last three decades, Antarctic SIE has shown a small, but significant increase during the same time period. However, in 2016, an unusually early onset of the melt season was observed; the maximum Antarctic SIE was already reached as early as August rather than end of September, and was followed by a rapid decrease. The decline of the sea ice area (SIA) started even earlier, namely in July. The decay was particularly strong in November where Antarctic SIE exhibited a negative anomaly (compared to the 1979-2015 average) of approximately 2 Mio. km^2, which, combined with reduced Arctic SIE, led to a distinct minimum in global SIE. ECMWF- Interim reanalysis data were used to investigate possible atmospheric influences on the observed phenomena. The early onset of the melt and the rapid decrease in SIA and SIE were associated with atmospheric flow patterns related to a positive ZW3 index, i.e. synoptic situations leading to strong meridional flow. Particularly, in the first third of November northerly flow conditions in the Weddell Sea and the Western Pacific triggered accelerated sea ice decay, which was continued in the following weeks due to positive feed-back effects, leading to the extraordinary low November SIE. In 2016, the monthly mean SAM index reached its second lowest November value since the beginning of the satellite observations. SIE decrease was preconditioned by

The Cryosphere Discuss., https://doi.org/10.5194/tc-2017-192
Manuscript under review for journal The Cryosphere
Discussion started: 22 September 2017
© Author(s) 2017. CC BY 4.0 License.

SIA decrease. A better spatial and temporal coverage of reliable ice thickness data is needed to assess the change in ice mass rather than ice area.

1 Introduction

Sea ice plays a critically important role in the cryosphere as well as the global climate system. It modifies heat, and mass exchange processes. Sea ice has a very high albedo compared to water, thus when present, it greatly increases the surface reflectivity. It also reduces the exchange of heat and moisture between the ocean and the lower atmosphere. Strong positive feedback effects related to sea ice changes have consequences for both atmosphere and ocean. Melting of sea ice rapidly decreases the surface albedo and increases turbulent heat exchange between ocean and atmosphere; it thus strongly influences the surface energy balance of the ocean (e.g. Stammerjohn, et al., 2012), which in turn affects sea ice itself. Formation and melt of sea ice also influences the sea water salinity by releasing salt (brine rejection) upon freezing and fresh water upon melting. These fluxes dominate the surface freshwater flux balance of the seasonally sea-ice covered Southern Ocean and thereby strongly influence the ocean overturning circulation (Haumann et al., 2016), which is critical for exchanging heat and carbon between the deep ocean and the atmosphere. Therefore, Antarctic sea ice plays an active role in the global climate system.

While in the Arctic the total sea ice extent (SIE) has been decreasing for more than three decades, Antarctic SIE has shown a small, but significant increase during the same time period (1.5 % per decade over the period 1979 to 2012), Turner et al., 2015), reaching record extents in 2013, 2014 and 2015 (e.g. Massonnet et al., 2015). However, in 2016, an unusually early onset of the seasonal ice melt was observed. The maximum Antarctic SIE was reached a month earlier, in August, rather than end of September, and was followed by rapid and continuous decrease until the summer when record minimum SIE was observed. The sea ice area (SIA), the total area actually covered by ice, started to exhibit values below the long-term average as early as July, with only a brief return to normal in late August when the general sea ice retreat began. The decay was particularly strong in November, when Antarctic SIE exhibited a negative anomaly (compared to the 1979-2015 average) of 1.84 Mio. km^2, which, combined with reduced Arctic sea ice, led to a distinct minimum in global SIE.

The present study is motivated by this unusual behaviour of Antarctic sea ice. Sea ice retreat, is influenced by atmospheric as well as oceanic processes. In this study we focus on the atmospheric influences on sea ice retreat and discuss possible reasons for the observed anomalous sea ice decay.

2 Previous work

The Cryosphere Discuss., https://doi.org/10.5194/tc-2017-192
Manuscript under review for journal The Cryosphere
Discussion started: 22 September 2017
© Author(s) 2017. CC BY 4.0 License.

Changes in sea ice can be induced by both atmospheric and oceanic processes. Locally, they can be caused by melting or freezing and by sea ice dynamics that influence ice advection, ice divergence and convergence (e.g. Enomoto and Ohmura, 1990). On a short time scale (days to weeks), both processes are strongly dependent on atmospheric influences, i.e. thermodynamics of the ocean-atmosphere interface and wind stress on the floating ice (e.g. Watkins and Simmonds, 2000). Oceanic influences mainly play a role on longer time scales, such as seasonal and interannual variations (e.g. Gordon, 1975; Martinson, 1990). In particular, while changes in the timing of sea ice retreat seem to have a strong influence on the timing of the following advance, advance and subsequent retreat are only weakly related (Stammerjohn et al., 2012). This suggests a strong oceanic thermal feedback that accelerates or decelerates autumn freeze onset (Stammerjohn et al., 2012). In a recent study, Su (2017) stated that the location of the sea ice edge at the SIE maximum is strongly correlated with the upper-ocean stratification in early winter (April-June). The seasonal influence of the ocean on sea ice extent has been the subject of a number of studies. Hall and Visbeck (2002) show that the strength and position of the westerlies influence northward Ekman transport and therefore the sea ice extent as well as upwelling of warmer water closer to the continent. This effect can cause stronger retreat of sea ice in summer, when the ice edge is farther south, and expansion of sea ice in winter (e.g. Lee et al., 2017).

Enomoto and Ohmura (1990) investigated the relationship of the sea ice edge advance/retreat and the semi-annual oscillation of the circumpolar trough. The ice drift depends on the position of the sea ice edge relative to the Antarctic convergence line (Enomoto and Ohmura (1990), which moves according to the semi-annual oscillation of the circumpolar trough (Meehl, 1991). This leads to ice divergence when the ice edge is north of the convergence and transport of ice towards the coast, when the ice edge is south of the Antarctic convergence line. The velocity of the ice drift amounts to 1-2% of the surface wind speed; the direction of the ice drift is turned by 10-40° to the left of the direction of the atmospheric flow, an average value of approximately 30° was found (Kottmeier et al, 1992, Nansen, 1902).Therefore, also zonal winds can have a substantial influence on the meridional ice transport and the SIE, particularly in the Ross and Weddell Seas (Haumann , 2011). Holland and Kwok (2012) investigated the influence of surface winds on Antarctic sea ice. They state that while in most parts of West Antarctica mainly wind-driven changes in ice advection are responsible for the observed SIC trends, wind-driven thermodynamic changes dominate in all other parts of the Southern Ocean. This means that both changes in the zonal and meridional components of the atmospheric circulation can induce sea ice anomalies, either through associated temperature anomalies or ice transport anomalies. Pezza et al. (2012) investigated the relationship between SIE and SAM/ENSO. They found that the relationship is not uniform for all longitudes and that the natural variability of SIE and SAM is so large that a longer reliable time series of sea ice and climate data would be necessary to establish a causal relationship between the two variables.

The Cryosphere Discuss., https://doi.org/10.5194/tc-2017-192
Manuscript under review for journal The Cryosphere
Discussion started: 22 September 2017
© Author(s) 2017. CC BY 4.0 License.

Usually, variations in the total Antarctic SIE are small since large contrasting regional variations, both positive and negative deviations from the mean, cancel each other. Large regional anomalies in SIC can be caused by stable synoptic situations, where atmospheric flow conditions that persist over several days or are dominant over several weeks lead to a southward (northward) ice transport combined with cold (warm) air advection (e.g. Massom et al., 2006, Schlosser et al., 2011). In a recent study, Turner et al. (2009) stated that the long-term increase in Antarctic SIE is mostly caused by an increase in the Ross Sea sector, which is strongly influenced by the strength and position of the Amundsen Sea Low (ASL) (Raphael et al., 2015). Turner et al. (2009) also related stratospheric ozone loss to the observed increase in Antarctic SIE and found that the strengthening of the westerlies, which is related to ozone depletion, deepens the ASL. They conclude, however, that the observed SIE increase might be still within the limits of natural variability.

Haumann et al. (2014) found that, on multidecadal time scales, changes in Antarctic SIE are linked to changes in the strength of meridional winds that are caused by a zonally asymmetric decrease in high-latitude surface pressure, the latter possibly being related to stratospheric ozone depletion or greenhouse gas increase. While increased southerly (and westerly) winds most likely fuelled the long-term increase of Antarctic sea ice over the satellite era, we here hypothesize that increased northerly winds and an associated warm air advection triggered the negative Antarctic sea ice anomaly in 2016.

Two recent studies investigated the observed unusually fast retreat in the spring of 2016. Turner et al. (2017), after a discussion of the climatological mean behaviour of Antarctic sea ice, consider the spatial differences of SIE anomalies and their temporal changes for five different sectors of the Southern Ocean. While in the Weddell Sea a marked change from positive to negative SIE anomalies occurred in November, the ABS and Indian Ocean showed mainly negative anomalies throughout the melt season. Ross Sea and West Pacific were exhibited both positive and negative SIE anomalies during the entire period. The decrease of SIE at a record rate is linked to record surface pressure anomalies, mainly in the Weddell Sea and Ross Sea sectors of Antarctica, and the related meridional flow and corresponding warm air advection (Turner et al., 2017). Alternatively, Stuecker et al. (2017) hypothesize that the anomalously low SIE in November-Dezember 2016 was largely related to positive SST anomalies due to the extreme El Nino event peaking in December-February (DJF) 2015/16 and the concurrent rather negative phase of the SAM.

Generally, changes in both oceanic and atmospheric processes could have been responsible for the observed 2016 anomaly. In the present study we investigated in detail the onset and temporal evolution of the sea ice retreat (considering both SIA and SIE as well as SIC) and the contributions of various parts of the Southern Ocean. A detailed analysis of the evolution of the SIA and SIE deficits shows a rapid growth of regional anomalies, suggesting an atmospheric origin of these changes. We compared those changes to ice drift data and related it to the general atmospheric flow conditions derived from

The Cryosphere Discuss., https://doi.org/10.5194/tc-2017-192
Manuscript under review for journal The Cryosphere
Discussion started: 22 September 2017
© Author(s) 2017. CC BY 4.0 License.

ECMWF interim-reanalysis and also considered the relationship to SAM and ZW3 indices and patterns.

2 Data and methods

2.1 Sea ice data

Sea ice data are provided by the National Snow and Ice Data Center (NSIDC). Sea ice concentrations (SIC) are derived from Nimbus-7 SMMR and DMSP SSM/I-SSMIS passive microwave data. The data set is generated from brightness temperature and designed to provide a consistent time series of sea ice concentrations. The data are provided in polar stereographic projection at a grid cell size of 25 km x 25 km. We use the Climate Data Record version 2 NASA Team algorithm (CDR NT) data for the period 1979 to 2015 as a baseline climatological record. These data are compared to the Near-Real-Time data (NRT; http://nsidc.org/data/NSIDC-0081) from January 2015 to June 2017, which are also derived from passive microwave data using the NASA Team algorithm. Days with a large number of missing pixels in the sea-ice area have been removed from the NRT data. The resulting SIE anomalies for the overlapping year 2015 agree well (Figure 1). To create monthly mean ice drift fields the low resolution sea ice drift product of the EUMETSAT Ocean and Sea Ice Satellite Application Facility (OSI SAF, www.osi-saf.org) were used.

Sea ice extent (SIE) is defined as the spatial sum of the area of grid boxes that have a sea ice concentration of at least 15%. Sea ice area is defined as the spatial sum of the sea ice concentration times the grid box area for grid boxes that have a sea ice concentration of at least 15%. The daily SIA change was computed by first calculating the daily SIA and then taking the difference in SIA from one day to the next. We computed daily and monthly anomalies as well as SIE and SIA deficits with respect to the climatological daily and monthly means of the CDR NT record over the period 1979 to 2015. Long-term trends shown in Figure 1 are computed using linear regression analysis.

2.2 ECMWF Re-analysis data

ECMWF Interim Re-analysis (ERA-Interim) data were employed to investigate atmospheric flow conditions. The re-analysis data are available from 1979 to today. The horizontal resolution is T255, corresponding to approximately 79 km. The model has 60 vertical levels, with the highest level being at 0.1hPa. A detailed description of ERA-Interim is given in Dee et al. (2011). We used monthly mean sea level pressure, derived from the daily mean values. The re-analysis data were used for investigation of ZW3 patterns and analysis of surface pressure fields and cyclone activity.

2.3 SAM and ZW3 indices

The Cryosphere Discuss., https://doi.org/10.5194/tc-2017-192
Manuscript under review for journal The Cryosphere
Discussion started: 22 September 2017
© Author(s) 2017. CC BY 4.0 License.

Meridional transport of heat and moisture in the high latitudes of the Southern Hemisphere is carried out by the asymmetric component of the circulation also known as quasi-stationary waves (Raphael, 2004). Together, zonal wave one (ZW1) and zonal wave three (ZW3) represent the largest proportion of this asymmetry (van Loon and Jenne, 1972). The asymmetry described by these zonal waves is revealed when the zonal mean is subtracted from the geopotential height field and coherent pattern of zonal anomalies and their associated flow become apparent. Both ZW1 and ZW3 have preferred regions of meridional flow, guiding the meridional transport of heat and moisture into and out of the Antarctic. ZW1 and ZW3 vary with each other so that when ZW3 is strong, ZW1 is weak and vice versa. An index of ZW3 based on its amplitude defined by Raphael (2004) shows that ZW3 has positive and negative phases where a positive phase indicates strong meridional flow and a negative phase more zonal flow. A climatology of this index shows that ZW3 tends to be negative from September through December, a period of time when ZW1 is dominant in the field (Raphael, 2004). Because it exerts control on the meridional flow, ZW3 influences the variability of Antarctic sea ice by dynamically and thermodynamically as illustrated in Raphael (2007).

The Southern Annular Mode (SAM) is the dominant mode of atmospheric variability in the extra-tropical Southern Hemisphere. Marshall (2003) calculated a SAM index based on the observed pressure difference between stations in Antarctica and at mid-latitudes. A large (small) meridional pressure gradient means a positive (negative) SAM index and, correspondingly strong (weak) westerlies. The stronger westerlies are usually connected to a more zonal flow, whereas in the case of a negative SAM index, the flow tends to meander in amplified Rossby waves. A positive SAM index is mostly related to positive SIC anomalies since, apart from the Antarctic Peninsula, air temperatures are lower due to decreased meridional heat exchange and the stronger westerlies can lead to increased northeastward transport of sea ice. A northerly flow during periods of negative SAM index can lead to compaction of the ice and/or melting due to warm air advection. The corresponding southerly flow means offshore flow, cold air advection and thus new ice formation. A negative SAM thus usually is associated with large regional differences in SIC and SIE anomalies. However, the SAM explains only approximately one third of the variability (Marshall, 2007) and there can be large regional differences for both the positive and the negative mode of SAM, e.g. strong zonal flow in the Pacific Ocean and strong meandering in the western Atlantic Ocean at the same time. In the present study we use the ZW3 and SAM indices to help explain the anomalous retreat of Antarctic sea ice in 2016.

3 Results

3.1 Temporal evolution of Antarctic sea ice extent and area

In Figure 1 monthly SIE anomalies from January 1979 to March 2017 are displayed. Until 2015, only relatively small variations and a generally positive trend can be seen. This trend is abruptly interrupted

The Cryosphere Discuss., https://doi.org/10.5194/tc-2017-192
Manuscript under review for journal The Cryosphere
Discussion started: 22 September 2017
© Author(s) 2017. CC BY 4.0 License.

in November 2016, when monthly mean SIE was almost 2 Mio. km^2 lower than in the preceding year. This value is clearly outstanding: the negative deviation from the mean reaches almost four times the standard deviation. Trends are calculated from the CDR data until 2015 and for the period including the most recent 15 months from NRT data, respectively. The extension of the period by these latter 15 months reduces the positive trend from 0.24 Mio. km^2 per decade to 0.17 Mio. km^2 per decade.

Figure 2 shows the daily Antarctic (SIE) (Fig. 2a) and sea ice area (SIA) (Fig. 2b) for the year 2016 together with the 1979-2015 average. The gray shading refers to the two standard deviations (1979-2015). While, on average, SIE extent increases until the end of September, in 2016, a sudden decrease occurred in the last third of August. After the first week of September, SIE fell below the long-term average and never recovered during the rest of the year. The anomaly in SIE increased from -0.1 Mio km^2 in August, to a maximum deviation from the mean of -1.84 Mio. km^2 in November. In December the anomaly amounted -2.33 Mio. km^2. The SIA exhibited negative deviations from the mean already in early July, briefly reached values close to the average again end of August and thereafter remained below the average for the rest of the year. The SIA anomaly for November and December 2016 are -1.98 Mio. km^2 and -1.55 Mio. km^2, respectively. The SIE deficit (shaded pink vs. dashed grey climatological average) also suggests that there were two distinct periods of decline, the first one in late August to mid-September, the second one in the first half of November. While the first period saw a corresponding decline in SIA, the second period is not as distinct for SIA. The overall largest SIA deficit of 2.24 Mio. km^2 occurred on 18 November, whereas the largest SIE deficit of 2.8 Mio. km^2 was seen approximately one month later, on 14 December. The sea ice did never recover in austral summer 2016/2017; in February 2017 the monthly mean SIE amounted to 2.27 Mio. km^2, which is the lowest value since beginning of the measurements. However, the monthly mean SIA was with 1.63 x 10^6 km^2 only the second lowest one, here the absolute minimum occurred in February 1993 (1.4 Mio. km^2).

In Figure 2c the SIA change (daily temporal derivative of the SIA) is shown. Again, the red and black lines refer to 2016 and the climatological mean (1979-2015), respectively. The SIA change can be interpreted as ice melt/compaction when it is negative and as new ice formation when it is positive. The pink shading indicates anomalously high melt or low freezing periods, the blue shading the opposite. A first, very short period with SIA decrease was observed as early as in mid-July when the SIA change assumed negative values for the first time.

It can be clearly seen that, until August, periods with growing and shrinking SIA deficit alternate, whereas from end of August on, almost only negative deviations from the mean are found, with negative SIA changes for the rest of the year. In addition to the periods mentioned above, a further period with strong sea ice decline can be seen in mid-October. During the general ice retreat, periods with accelerated decline alternate with periods that exhibit a decline slower than on average.

The Cryosphere Discuss., https://doi.org/10.5194/tc-2017-192
Manuscript under review for journal The Cryosphere
Discussion started: 22 September 2017
© Author(s) 2017. CC BY 4.0 License.

240

3.2 Regional sea ice changes

3.2.1 SIC anomalies and corresponding influence of cyclonic activity

To investigate, which areas contributed most strongly to the observed changes, Antarctica was divided into seven sub-areas (see Table 1), the definition following the regional SIC anomalies displayed in
245 Fig. 3 for the months August to November 2016. This division is finer than the five sub-areas used in previous studies (.e.g. Turner et al., 2017). The SIC anomalies, as usual, exhibit strong regional differences, areas with positive deviations alternating with areas of negative deviations. In August, the total SIE is only 0.1 Mio km^2 smaller than the long-term average (1979-2015). The contributions of areas with negative anomalies mostly counteract those of areas with positive anomalies. Largest
250 negative anomalies are found at the edge of the Eastern Weddell Sea and in the Western Indian Ocean, where also the sea ice edge is already distinctly farther south than on average. In the Western Pacific, only a very small area, centered at approximately130 °E shows negative deviations, otherwise SIE is very close to the mean value, SIC anomalies are slightly positive. In the Western Ross Sea, SIE is also close to the long-term average; positive deviations in SIC are found near 150°E and at the northern
255 edge of the Ross Sea. The Amundsen and Bellingshausen Seas have smaller negative deviations from the mean SIE than the Indian Ocean, whereas the Weddell Sea exhibits positive SIC anomalies between approximately 35°W and 0°, associated with a sea ice edge farther north than on average.

Generally, SIC depends on ice dynamics (advection) and thermodynamics, both, on short time scales, being strongly influenced by the atmospheric flow. Figure 6 shows the monthly mean surface pressure
260 for the corresponding months. Arrows indicate the main surface flow related to changes in SIC or SIE. In the Southern Hemisphere, the air circulates clock-wise around the center of a cyclone, meaning a northerly (southerly) flow at the western (eastern) flank of the cyclone. Northerly flow leads to compaction of the ice and/or advection of warmer air, thus reducing the SIE by compaction and/or melt, whereas a southerly flow is related to northward drift of the ice and formation of new ice close to
265 the coast due to cold air advection from the continent over leads and polynyas that develop as the ice is pushed away. The strong westerly flow at the northern edge of the cyclone can, via Ekman transport (e.g Hall and Visbeck, 2001), also lead to net northward transport of sea ice and thus an increase in SIE.

In August (Figure 4a), the Amundsen-Bellingshausen Sea Low, in the following called Amundsen Sea
270 Low (ASL), was replaced by an extended cyclone centered above the eastern Ross Sea, the strong southerly flow at its western flank leading to the positive SIC concentrations in eastern R4, correspondingly the northwesterly flow at its eastern flank causing negative SIC anomalies in R5 and in the Amundsen-Bellingshausen Seas (R6). The small, but distinct negative SIC anomaly east of 120°E is related to a low pressure system in the Eastern Indian/Western Pacific Ocean, that steered

© Author(s) 2017. CC BY 4.0 License.

relatively warm air masses from areas north of 55°S right towards the mentioned anomaly. The area is rather restricted due to the confluent flow. In the Eastern Weddell Sea (R1) and the Western Indian Ocean (R3), there was a weak, but extended low pressure system, that caused a weak northerly flow towards the western edge of R2 associated with the negative SIC anomalies. However, most of the R2 was under the influence of a very weak pressure gradient, and consequently no distinct flow conditions prevailed.

In September (Figure 4b), positive SIC anomalies occurred in R1, R3, and R5. The area with negative anomalies just east of 120°E extended across the entire R4. Additionally, SIC anomalies in R6, and R7 were largely negative. The low pressure system in the Pacific Ocean intensified and moved eastwards, extended across the Ross and Bellingshausen Seas which resulted in positive (negative) SIC anomalies at its western (eastern) flank. While R4 was still influenced by the low centered in R3, the positive anomalies in R3 cannot be explained by this low since warm air advection would be expected here. Similarly, the negative SIC anomalies between 180°W and approximately 160°E are unexpected since this area is influenced by the Pacific low. In the northern parts of the Eastern Weddell Sea, positive SIC anomalies are observed, possibly related to the strong westerly flow resulting in north-eastward Ekman transport.

In October (Figure 4c), the SIC anomalies occurred in the same areas as in September, but were more strongly developed. The ASL stretched eastward and is now true to its name and extended across the Amundsen and Bellingshausen Seas. In the Eastern Weddell Sea a strong low pressure system has developed, leading to a northerly flow in the Western Indian Ocean, where strong negative SIC anomalies are observed. The Western Pacific low extended northwards, although with a weaker pressure gradient. SIE in R3 changed very little and slightly less negative SIC concentrations occurred. The negative anomaly in SIE of R2 remained nearly constant in September and October.

In November (Figure 4d), R2 exhibited strong negative anomalies in SIE and SIC, which contributed to the melt period in the first half of November (Fig. 2c). Also large negative deviations from mean SIC occurred in the Eastern Pacific (R4), the Amundsen and Bellingshausen Seas (R6), and in the western Weddell Sea (R7), whereas strong positive deviations in SIC were found in the Eastern Weddell Sea and Lazarev Sea (R1),and the eastern Ross Sea (R5).

Note that we are considering monthly means here. A signal that is still visible in a monthly mean has to have been predominant over the majority of days during that month or has to have been very strong over a shorter time period (shorter time periods). The latter was the case at the end of August, and also in November: in the first third of the month the prevailing northerly flow was very strong and thus crucial for triggering the increased melt. This is shown in Figure 6e, where the mean sea level pressure for 1- 10 November 2016 is displayed. Between an extended low pressure system above the Western Pacific and a high pressure ridge in the Western Ross Sea a strong northerly flow with warm air

© Author(s) 2017. CC BY 4.0 License.

advection is related to the large negative SIC anomalies in that area. Equally, in the western and central Weddell Sea, a northerly flow at the eastern flank of a low pressure system is associated with strong negative SIC anomalies. In the Western Indian Ocean, the picture is not as straightforward; oceanic memory effects may play a role here.

Summarizing, the observed regional SIC anomalies in spring 2016 can to a large extent be explained by the atmospheric flow related to unusually strong and persistent low pressure systems leading to strong warm air advection from northerly directions and thus increased ice melt.

3.2.2 Temporal evolution of regional SIE and SIA

To get a deeper insight into the spatial origin of the anomalies in SIE and SIA, in Fig. 5 the daily values of SIC, SIA, and SIA changes are displayed (similar to Fig. 2, for details see Figure caption) for the different regions 1-7 shown in the respective maps. Regions 3 and 5 did not contribute to the accelerated sea ice decay. They have predominantly positive anomalies in SIE, SIA and SIC. Regions R1, R4 and R7 contributed to the negative SIE and SIA anomalies through strong events caused by the corresponding atmospheric flow discussed above, whereas R2 and R6 exhibited more or less continuous negative deviations from the long-term mean. This is most clearly seen in the respective deficits of SIE and SIA shown at the bottom of the Fig. 5 plots. In R1, both SIA and SIE stayed above the long-term average, but contributed strongly to the negative anomaly through a distinct event in November.

The first slightly negative changes in SIA in mid-July occurred only in the Western Pacific (R4) and in the Amundsen Bellingshausen Seas (R6). The start of the melt period end of August is also seen here. The Western Indian Ocean (R2) exhibited negative SIE and SIC anomalies, even though the SIA change hinted at anomalously high freezing in this area at the end of August. The negative anomalies in this area might be an oceanic memory effect since the area showed similar features in the preceding year (not shown here). The two regions R4 and R6 also most strongly contributed to the continuation of the late August melting into the first half of September. The Weddell Sea (R1 and R7) did not contribute significantly to the sea ice decay in these early periods. In mid-September/October, the contribution of the Western Weddell Sea increased, whereas the Eastern Weddell Sea/Lazarev Sea contributed late, but strongly from mid-November into December to the negative sea ice anomalies.

3.2.3 Ice drift

Ice drift influences SIE, SIA and SIC in various ways. For SIC below 100%, northerly winds lead to sea ice compaction. Southerly winds imply offshore winds that can cause coastal polynyas. These

© Author(s) 2017. CC BY 4.0 License.

polynyas are usually quickly closed by new ice formation due to associated cold air advection from the continent. Strong westerly winds lead to net north-eastward Ekman transport. Apart from that, convergence/confluence and divergence/diffluence in the main atmospheric flow can locally change SIC.

Since sea ice drift is strongly influenced by surface winds, we examine the monthly mean ice motion from August to November 2016, illustrated in Fig. 6. It shows generally good agreement with the sea level pressure fields shown in Fig. 4, taking into consideration the corresponding wind fields discussed in 3.2.1. Only in areas where SIE is already small, i.e. in R3 and the eastern half of R6 in October and November, the correlation between ice drift and wind direction more or less disappears due to the low resolution of the plotted ice drift. In August, the large low pressure system above the Weddell and Lazarev Seas is associated with clockwise ice drift in the Weddell Sea and drift towards the continent at its eastern flank. With increasing pressure gradient in September, the movement increases at the northern flank, whereas the southward drift at its eastern flank disappears due to a predominantly westerly flow in the Lazarev Sea. The ice drift connected to the ASL is best developed in September, with strong southerly (northwesterly) flow at the western (eastern) flank of the cyclone.

In November, similar to the SIC anomalies, the first third of the month is crucial for the monthly mean sea ice drift. The direction and strength of the ice drift is strongly connected to the average sea level pressure field for Nov 1st to 10th, shown in Fig. 4e. The patterns of the strong clockwise circulation in the Western Weddell Sea, leading to compaction and ice melt, thus quickly decreasing SIC, the drift towards the coast in the Western Pacific (negative SIC anomaly) and the offshore drift in the Western Ross Sea, connected to the positive SIC and SIE anomaly, can be clearly related to the pressure field and the corresponding surface winds.

3.3 General atmospheric flow conditions during the melt season 2016/17

After having investigated in section 3.2.1 the local meridional atmospheric flow related to sea ice changes specificly for individual low pressure systems (cyclones) observed during the melt period, we now want to consider the large-scale general atmospheric flow conditions.

3.3.1 ZW3

The monthly mean sea level pressure shown in Fig. 4 has a clear signal of ZW3, most strongly in August and October. Given this, we examine the ZW3 index for the period of ice decay. Figure 7a shows the daily ZW3 index for 2013-2016. Clearly, 2016 shows a distinctly different picture from the preceding years 2013-2015. However, the largest differences occur in the cold season, namely mid-April to June, and, with short interruptions, well into August. In 2016, the positive ZW3 index is

© Author(s) 2017. CC BY 4.0 License.

predominant from mid-April far into July and, with short interruptions, until mid-October. The sudden and unexpected decrease in SIE at the end of August comes after a prolonged period of positive ZW3 indices, whereas in November, when the record minimum SIE was observed, the ZW3 index is highly variable, both positive and negative.

Since an increased meridional exchange can also be related to ZW1 we looked at the 500hPa geopotential height anomaly shown in Fig. 7b. It is created by subtracting the long-term zonal mean at each latitude, from the mean 500-hPa geopotential height field in November 2016, thus elucidating the asymmetry in the circulation suggested by the index. In August, as expected from the sign of the ZW3 index and the mean sea level pressure distribution in Fig. 6a, a distinct ZW3 pattern can be seen, leading to fairly strong meridional flow and thus meridional heat exchange in the respective areas described in section 3.2.1. While in September the pattern is disturbed in the Atlantic sector (no distinct meriodional flow, see Fig. 4b), in October it reappeared, but was no longer as well-defined as in August. In November, while no clear ZW3 pattern is found, a distinct meridional flow can be seen around the Ross Sea and in the Weddell Sea in the first third of the month (see Fig. 4e). A clear ZW3 pattern is not expected here since the amplitude of the wave as shown in Fig. 7a is negative for most of the month. However, while a positive ZW3 index is not coincident with the decrease in November, its persistence in the preceding months will have preconditioned the ice so that the effect of any other activity that promotes ice loss would be amplified. The flow pattern associated with the strong negative anomaly in the 500hPa geopotential height above the Weddell Sea is consistent with the strong melt there due to warm air advection from the north.

3.3.2 Southern Annular mode

Figure 8 shows the monthly mean SAM index based on the calculation of Marshall (2003) for 2016 and the climatological monthly means calculated for the period 1979-2015. In November, the months with the largest ice loss, the SAM index is highly negative, in fact, the second lowest SAM index since the start of the satellite sea ice observations occurred. This would suggest a rather meridional flow resulting in comparatively large meridional exchange of heat and moisture. Different from ZW3, which has been strongly positive already from May on and continuing during the entire winter months, thus hinting at increased meridional flow, the SAM index is positive in most months. However, as mentioned above, it should be kept in mind that SAM explains only part of the variability of the circulation, and large regional differences in the flow pattern can occur. Additionally, the monthly means are not always meaningful since periods with positive and negative indices can cancel each other.

The Cryosphere Discuss., https://doi.org/10.5194/tc-2017-192
Manuscript under review for journal The Cryosphere
Discussion started: 22 September 2017
© Author(s) 2017. CC BY 4.0 License.

4 Discussion and conclusion

The record minimum in Antarctic SIE in November 2016 was associated with an unusually early start of the melt season with negative anomalies in SIA (SIE) observed as early as July (August). Although other components of the climate system, such as the ocean must have contributed to this anomalous melt, our analysis suggests that increased meridional heat exchange with middle latitudes due to strongly meandering westerlies played a significant role. This is expressed by a persistently positive ZW3 index, a measure of the meridionality of the flow, during most of the winter and early spring. The influence of ZW3 is reduced in November, whereas the phase of the SAM was strongly negative, its index reaching an almost record negative value. The first third of November was under the influence of strong warm air advection in the areas with negative sea ice anomalies. This relatively short, but intense period triggered the accelerated ice melt melt, which was being continued in the following weeks due to the positive feed-back effects of the ice melt, i.e. lower albedo of the open vs ice-covered ocean and increased turbulent heat flux from the ocean. The timing of this triggering was crucial for the increased melt; it happened exactly at the height of the melt season when conditions were set for melt anyway (strong radiation, high air temperatures). Our results agree well with the general findings of Turner et al. (2017). While they stress the comparison of conditions in 2016 with the climatological means of amount and timing of SIE minima and maxima as well as mean location and intensity of cyclones, our study looks more closely at both SIA and SIE, investigates the contribution of the different parts of the Southern Ocean to ice melt in more detail, discusses the role of ice drift and the relationship between sea ice decay and SAM and ZW3.

Distinct melt periods were observed at the end of August, in the first half of September, in mid-October and in the first half of November. Three main areas of ice loss are found: The Amundsen-Bellingshausen Seas, the Western Indian Ocean and the Eastern Pacific/Western Ross Sea. This loss is only partly counteracted by a positive anomaly in SIE off Marie Byrd Land, east of the Ross Sea (centred at approx. 130°W) and at the northern edge of the Weddell Sea. In November, also the Weddell Sea strongly contributed to the accelerated sea ice retreat. The strong melting in the Amundsen-Bellingshausen Seas was caused by an extended and eastward-shifted ASL and consequent warm air advection at its eastern flank. The Western Indian Ocean exhibits negative anomalies in SIE and SIC, however, they do not increase significantly before November. The positive feedback mechanisms mentioned above further accelerated the sea ice decay.

The thermodynamic influence of atmospheric flow patterns described by positive ZW3 indices and negative SAM indices results in increased ice melt only close to and in the melt period, i.e. when the air masses advected from the north have temperatures above the freezing point. A comparison of July SIE in the years 2009 and 2010, which had extremely different flow conditions (Schlosser et al., 2015) shows no significant difference in total SIE, even though 2010 had extremely zonal flow conditions, whereas 2009 exhibited strong amplification of Rossby waves with increased meridional heat

© Author(s) 2017. CC BY 4.0 License.

exchange. In winter, atmospheric flow patterns are not sufficient to cause increased ice melt, since air temperatures are generally too low to cause ice melt, in spite of strong "warm" air advection.

Compaction of the ice by northerly atmospheric flow is only efficient if the SIC is clearly lower than 100%. In winter, in this case the compaction of the ice leads to formation of new ice at the ice edge, which is thinner and has a lesser snow cover than the ice formed early in the winter and thus can be melted rapidly as soon as temperatures get sufficiently high. The persistently positive ZW3 indices from mid-April to June (Fig. 7a) suggest that in 2016 the sea ice underwent the described preconditioning due to compaction. This is also supported by the early decline in SIA in July.

In the Northern Weddell Sea, positive SIC anomalies are found far into the melt season. These are probably mainly caused by ice dynamics rather than thermodynamics, the strong westerlies in that area causing ice divergence and thus northeastward transport of the ice. Supporting thermodynamical influence is found in August and October, where a southerly flow with cold air advection from the continent prevailed at the western flank of a distinct low pressure system centered at the eastern border of the Weddell Sea.

The results presented here are so far mostly qualitative. A regional atmospheric flow model combined with surface energy balance modelling would be necessary to quantify the ice melt in dependence on available energy due to warm air advection. The present study is focussed on the atmospheric influence on the sea ice behaviour in the melt season of 2016. The oceanic influence usually has longer time scales and reaction times, but cannot be neglected. Even though the memory effect is more important for the formation than for the melt of sea ice (Stammerjohn et al., 2012), there might be processes on a larger time scale that play a role here, too. Our results suggest that the exceptional sea ice conditions in 2016 are owing to a superposition of serveral events in different parts of the Southern Ocean. It remains to be seen how fast the Antarctic sea ice recovers from the unusual conditions in 2016 and whether those conditions will influence sea ice in the following year.

Acknowledgements

This study was financed by the Austrian Science Fund (FWF) under grant P28695. Sea ice data were provided by the NSIDC (National Snow and Ice Data Center), Boulder, CO (ftp://sidads.colorado.edu/DATASETS/NOAA/G02135/south/monthly/data/). ECMWF is greatly appreciated for the Interim-reanalysis data (https://www.ecmwf.int/en/research/climate-reanalysis/era-interim). We are grateful to Gareth Marshall (BAS) for online provision of the observation-based SAM index (https://legacy.bas.ac.uk/met/gjma/sam.html).

© Author(s) 2017. CC BY 4.0 License.

480

Author contribution:

The scientific analysis was jointly done by all authors, ES wrote the manuscript with contributions of MR and AH; MR performed the ZW3 analysis, and AH carried out all other calculations and graphics.

485 **References**

Cavalieri, D. J., C. L. Parkinson, P. Gloersen, and H. J. Zwally: updated yearly. *Sea Ice Concentrations from Nimbus-7 SMMR and DMSP SSM/I-SSMIS Passive Microwave Data, Version 1*. [Indicate subset used]. Boulder, Colorado USA. NASA National Snow and Ice Data Center Distributed Active Archive
490 Center. doi: http://dx.doi.org/10.5067/8GQ8LZQVL0VL. [Date Accessed], 1996.

Dee, D. P., and 34 others: The ERA-Interim reanalysis: configuration and performance of the data assimilation system. Q. J. Roy. Met. Soc. 137, 553-597, doi:10.1002/qj828, 2011.

Enomoto, H. and A. Ohmura: 1990. The influences of atmospheric half-yearly cycle on the sea ice extent in the Antarctic. J. Geophys. Res., 95 (C6), 9497–9511.

495

Gordon, A. L., and H. W. Taylor: Seasonal change of Antarctic Sea Ice Cover. Science, 187 (4174), 346-347, 1975.

Hall, A. and M. Visbeck: Synchronous Variability in the Southern Hemisphere Atmosphere, Sea Ice,
500 and Ocean Resulting from the Annular Mode. *J. Climate*, **15**, 3043–3057, https://doi.org/10.1175/1520-0442(2002)015<3043:SVITSH>2.0.CO;2, 2002.

Haumann, F. A.. Dynamical Interaction between Atmosphere and Sea Ice in Antarctica. Master's thesis. Utrecht University, 141pp, 2011.

505

Haumann, F. A., D. Notz and H. Schmidt: Anthropogenic influence on recent circulation-driven Antarctic sea-ice changes. Geophysical Research Letters. doi:10.1002/2014GL061659, 2014.

Haumann, F. A.**,** **N**. Gruber, M. Münnich, I. Frenger, S. Kern: Sea-ice transport driving Southern Ocean salinity and its recent trends. Nature, 537, 89–92. doi:10.1038/nature19101, 2016.

510 Hobbs, W. R., R. Massom, S. Stammerjohn, P. Reid, G. Williams, and W. Meier. A review of recent changes in Southern Ocean sea ice, their drivers and forcings. Glob. Planet. Change, 143, 228-250, https://doi.org/10.1016/j.gloplacha.2016.06.008, 2016.

© Author(s) 2017. CC BY 4.0 License.

Holland, P.R. and R. Kwok: Wind-driven trends in Antarctic sea-ice drift. Nature Geoscience, 1-4, doi:10-1038/NGEO1627, 2012.

Kottmeier, C., J. Olf, W. Frieden, and R. Roth: Wind Forcing and Ice Motion in the Weddell Sea Region. J. Geophys. Res., 97(D18), 20,373-20,383, 1992.

Kottmeier, C., and L. Sellmann: Atmospheric and oceanic forcing of Weddell Sea ice motion. J. Geophys. Res., 101(C9), 20,809-20,824, 1996.

Marshall, G. J.: Trends in the Southern Annular Mode from observations and reanalyses, J. Clim., 16, 4134-4143, 2003.

Marshall, G. J. : Half-century seasonal relationship between the Southern Annular Mode and Antarctic temperatures, Int. J. Climatol., 27, 373-383, 2007.

Martinson, D. G.: Evolution of the Southern Ocean Winter Mixed Layer and Sea Ice: Open Ocean Deep Water Formation and Ventilation. J. Geophys. Res., 95 (C7), 11,641-11,654, 1990.

Maslanik, J. and J. Stroeve: *Near-Real-Time DMSP SSMIS Daily Polar Gridded Sea Ice Concentrations, Version 1*. [Indicate subset used]. Boulder, Colorado USA. NASA National Snow and Ice Data Center Distributed Active Archive Center. doi:http://dx.doi.org/10.5067/U8C09DWVX9LM, updated daily. [Accessed July 3, 2017], 1999.

Massom, R., S. E. Stammerjohn, R. C. Smith, M. J. Pook, R. A. Iannuzzi, N. Adams, D. G. Martinson, M. Vernet, W. R. Fraser, L. B. Quetin, R. M. Ross, Y. Massom, and H. R. Krouse: Extreme Anomalous Atmospheric Circulation in the West Antarctic Peninsula Region in Austral Spring and Summer 2001/02, and Its Profound Impact on Sea Ice and Biota. J. Climat.., 19, 3544-3571, http://dx.doi.org/10.2275/JCLI3805.s1, 2006.

Massonnet, F., V. Guemas, N. S. Fuckar, and F. J. Doblas/Reyes: The 2014 high record of Antarctic sea ice extent. In: Herring, S. C., M. P. Hoerling, J. P. Kossin, T. C. Peterson, and P. A. Scott (eds.): Explaining extreme events of 2014 from a climate persperctive. Special supplement to the Bull. Amer. Meteor. Soc., 96, 163-167, doi:10.1175/BAMS-D-15-00093.1, 2015.

Meehl, G. A: Reexamination of the Mechanism of the Semiannual Oscillation in the Southern Hemisphere. J. Climat., 4, 911-926, 1991.

Meier, W., F. Fetterer, M. Savoie, S. Mallory, R. Duerr, and J. Stroeve: NOAA/NSIDC Climate Data Record of Passive Microwave Sea Ice Concentration, Version 2. Boulder, Colorado USA: National Snow and Ice Data Center. http://dx.doi.org/10.7265/N55M63M1, 2013, updated 2016.

© Author(s) 2017. CC BY 4.0 License.

Nansen, F. :The Oceanography of the North Polar Basin, the Norwegian North Polar Expedition 1893-1896. Scientific Results, Vol. 3, Kristiania, 427pp, 1902.

Peng, G., W. Meier, D. Scott, and M. Savoie: A long-term and reproducible passive microwave sea ice concentration data record for climate studies and monitoring, Earth Syst. Sci. Data. 5. 311-318. http://dx.doi.org/10.5194/essd-5-311-2013, 2013.

Pezza, A. B. , H. A. Rashid, and I. Simmonds: Climate links and recent extremes in antarctic sea ice, high-latitude cyclines, Southern Annular Mode and ENSO. Clim. Dyn., 38:57-73, doi:10.1007/s00382-011-1044-y, 2012.

Raphael, M. N.: A zonal wave 3 index for the Southern Hemisphere, Geophys. Res. Let., 31(23), doi:10.1029/2004GL020365, 2004.

Raphael, M. N., G. J. Marshall, J. Turner, R. L. Fogt, D. Schneider, D. A. Dixon, J. S. Hosking, J. M. Jones, and W. R. Hobbs: The Amundsen Sea Low. Variability, Change, and Impact on Antarctic Climate. *Bull. Am. Meteorol. Soc.* **97,** 111–121, doi: 10.1175/BAMS-D-14-00018.1, 2015.

Schlosser, E.**:** Optical Studies of Antarctic sea ice. *Cold Regions Science and Technology*, **15**, 289-293, 1988.

Schlosser, E., J. G. Powers, M. G. Duda, K. W. Manning:. Interaction between Antarctic sea ice and synoptic activity in the circumpolar trough – implications for ice core interpretation, Ann. Glaciol., **52** (57) 9-17 , 2011.

Schlosser, E., Stenni, B., Valt, M., Cagnati, A., Powers, J. G.,Manning, K. W., Raphael, M., and Duda, M. G.: Precipitation and synoptic regime in two extreme years 2009 and 2010 at Dome C, Antarctica – implications for ice core interpretation, Atmos. Chem. Phys., 16, 4757–4770, doi:10.5194/acp-16-4757- 2016, 2016.

Simmonds, I., Keay, K., and Lim, E.: Synoptic activity in the seas around Antarctica. Mon. Wea. Rev., 131, 272-288, 2002.

Simmonds, I.: Comparing and contrasting the behaviour of Arctic and Antarctic sea ice over the 35-year period 1979-2013. Ann. Glaciol., 56, 18-28, doi:10.3189/2015AoG69A909, 2015.

Stammerjohn, S., R. Massom, D. Rind, D. Martinson: Regions of rapid sea ice change: An inter-hemispheric seasonal comparison. Geophys. Res. Lett., 39, L06501, doi:10.1029/2012GL050874, 2012.

© Author(s) 2017. CC BY 4.0 License.

Stuecker, M. F., C. M. Bitz, and K.C. Armour: Conditions leading to the unprecedented low Antarctic sea ice extent during the 2016 austral spring season. Geophys. Res. Lett., 2017.

Turner, J., J. C. Comiso, G. J. Marshall, T. A. Lachlan-Cope, T. Bracegirdle, T. Makszm, M. P. Meredith, Z. Wang, A. Orr: Non-annular atmospheric circulation change induced by stratospheric ozone depletion and its role in the recent increase of Antarctic sea ice extent. Geophys. Res. Lett., 36 (8), doi:10.1029/2009GL037524, 2009.

Turner, J., J. S. Hosking, T. J. Bracegirdle, G. J. Marshall, and T. Phillips: Recent changes in Antarctic sea ice. Phil. Trans. R. Soc. A373: 20140163. http://dx.doi.org/10.1098/rsta.2014.0163, 2014.

Turner, J., J. C. Comiso, G. J. Marshall, T. A. Lachlan-Cope, T. Bracegirdle, T. Maksym, M. P. Meredith, Z. Wang, and A. Orr: Non-annular atmospheric circulation change induced by stratospheric ozone depletion and its role in the recent increase of Antarctic sea ice extent. Geophys. Res. Lett., 36, L08502, doi:10.1029/2009GL037524, 2009.

Turner, J., T. Phillips, G. J. Marshall, J. Scott Hosking, J. O. Pope, T. J. Bracegirdle, and P. Deb: Unprecedented springtime retreat of Antarctic sea ice in 2016. Geophys. Res. Lett., doi:10.1002/2017GL073656, 2017.

Van Loon, H., and Jenne, R. L.: The zonal harmonic standing waves in the Southern Hemisphere, J. Geophys. Res., 77, 992-1003, 1972.

Watkins A. B. and I. Simmonds: Current trends in Antarctic Sea ice: The 1990s impact on a short climatology. J. Climate, 13, 4441-4451, https://doi:.org/10.1175/1520-0442(2000)013<4441:CTIASI>2.0.CO:2, 2000.

The Cryosphere Discuss., https://doi.org/10.5194/tc-2017-192
Manuscript under review for journal The Cryosphere
Discussion started: 22 September 2017
© Author(s) 2017. CC BY 4.0 License.

Table 1.

Regions used for the regional analysis (Fig. 5).

R1	Eastern Weddell Sea / Lazarev Sea	20°W - 25° E
R2	Western Indian Ocean	25°E - 85° E
R3	Eastern Indian Ocean	85°E - 130° E
R4	Western Pacific / Western Ross Sea	30°E - 155° W
R5	Eastern Ross Sea	155°W - 125° W
R6	Amundsen-Bellingshausen Seas	25°W - 60° W
R7	Western Weddell Sea	60°W - 20° W

610

615

620

625

The Cryosphere Discuss., https://doi.org/10.5194/tc-2017-192
Manuscript under review for journal The Cryosphere
Discussion started: 22 September 2017
© Author(s) 2017. CC BY 4.0 License.

Figure captions

630

Fig. 1

Monthly mean sea ice extent (SIE) anomalies since 1979 with respect to the 1979 to 2015 climatology. The period 1979 through 2015 is derived from the Climate Data Record NASA Team (CDR NT) data (green; Meier et al., 2013, updated 2016; provided by NSIDC). The period January 2015 through June 635 2017 is derived from the Near Real Time (NRT) data (red; Maslanik and Stroeve, 1999, updated daily; provided by NSIDC). Green shading shows the ±2 standard deviation of the CDR NT record and the green dashed line the respective long-term trend derived from linear regression analysis. The red dashed line shows the long-term trend for the period 1979 through June 2017 when extending the CDR NT record using the period January 2016 through June 2017 from the NRT record.

640

Fig. 2

Seasonal cycle of the daily (a) sea ice extent (SIE), (b) sea ice area (SIA), and (c) sea ice area change, calculated as the temporal derivative of SIA. The black lines show the climatological mean daily values for the period 1979 through 2015 derived from the Climate Data Record NASA Team (CDR 645 NT) data (Meier et al., 2013, updated 2016; provided by NSIDC). The red lines show daily values for the year 2016 derived from the Near Real Time (NRT) data (red; Maslanik and Stroeve, 1999, updated daily; provided by NSIDC). (a and b) Grey shading shows the ±2 standard deviations of the CDR NT record and red shading the deficit of the year 2016 with respect to the CDR NT record. **(c)** Positive (negative) SIA change is associated with a gain (loss) of SIA. Red and blue shading indicate periods in 650 which the 2016 SIA deficit was growing and shrinking, respectively, with respect to the 1979 to 2015 period. The dashed line indicates the ±1 standard deviation of the CDR NT record.

Fig. 3

Monthly mean sea ice concentration anomalies for the months August to November 2016 (a to d) 655 derived from the Near Real Time (NRT) data (red; Maslanik and Stroeve, 1999, updated daily; provided by NSIDC). Anomalies are calculated with respect to the climatological monthly mean derived from the Climate Data Record NASA Team (CDR NT) data from the period 1979 through 2015 (Meier et al., 2013, updated 2016; provided by NSIDC). Regions for the regional analysis (Fig. 4) are indicated by the black lines and defined in Table 1.

660

© Author(s) 2017. CC BY 4.0 License.

Fig. 4

Monthly mean sea level pressure a) August, b) September, c) October, d) November 2016, and e) mean sea level pressure 1 – 10 Nov 2016. Arrows indicate the main atmospheric flow direction related to ice drift and SIC anomalies (Data from ECMWF Interim-Reanalysis)

Fig. 5

As Figure 2, but for each of the seven regions separately. Regions are indicated in the inset map and Figure 3, and are defined in Table 1.

Fig. 6

Monthly mean sea ice drift (arrows) for the months August to November 2016 (a to d) derived from the low resolution sea ice drift product of the EUMETSAT Ocean and Sea Ice Satellite Application Facility (OSI SAF, www.osi-saf.org; Lavergne, et al., 2010). White shading shows the respective monthly mean sea ice concentration derived from the Near Real Time (NRT) data (red; Maslanik and Stroeve, 1999, updated daily; provided by NSIDC). The grey contour line shows the 15% sea ice concentration line.

Fig. 7

a) Daily Zonal Wave Number 3 (ZW3) index 2013 - 2016

b) Monthly 500hPa geopotential height zonal mean anomalies Aug – Nov 2016

Fig. 8

Monthly mean SAM index for 2016 and climatological monthly mean SAM index 1979-2015 (after Marshall, 2003)

The Cryosphere Discuss., https://doi.org/10.5194/tc-2017-192
Manuscript under review for journal The Cryosphere
Discussion started: 22 September 2017
© Author(s) 2017. CC BY 4.0 License.

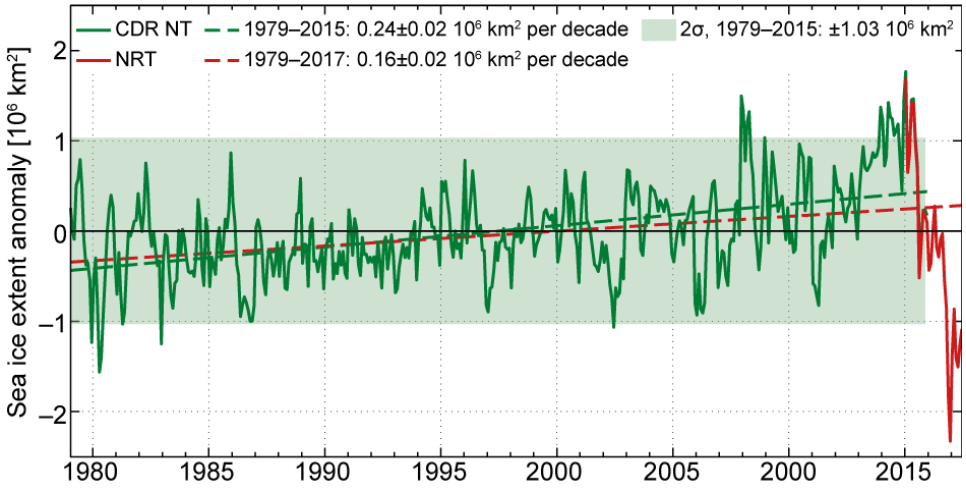

Fig. 1

The Cryosphere Discuss., https://doi.org/10.5194/tc-2017-192
Manuscript under review for journal The Cryosphere
Discussion started: 22 September 2017
© Author(s) 2017. CC BY 4.0 License.

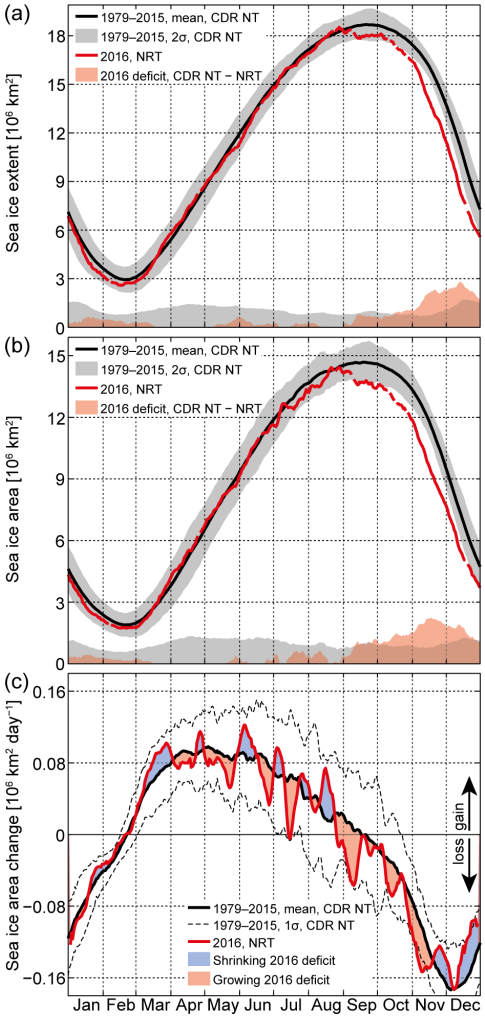

Fig. 2

The Cryosphere Discuss., https://doi.org/10.5194/tc-2017-192
Manuscript under review for journal The Cryosphere
Discussion started: 22 September 2017
© Author(s) 2017. CC BY 4.0 License.

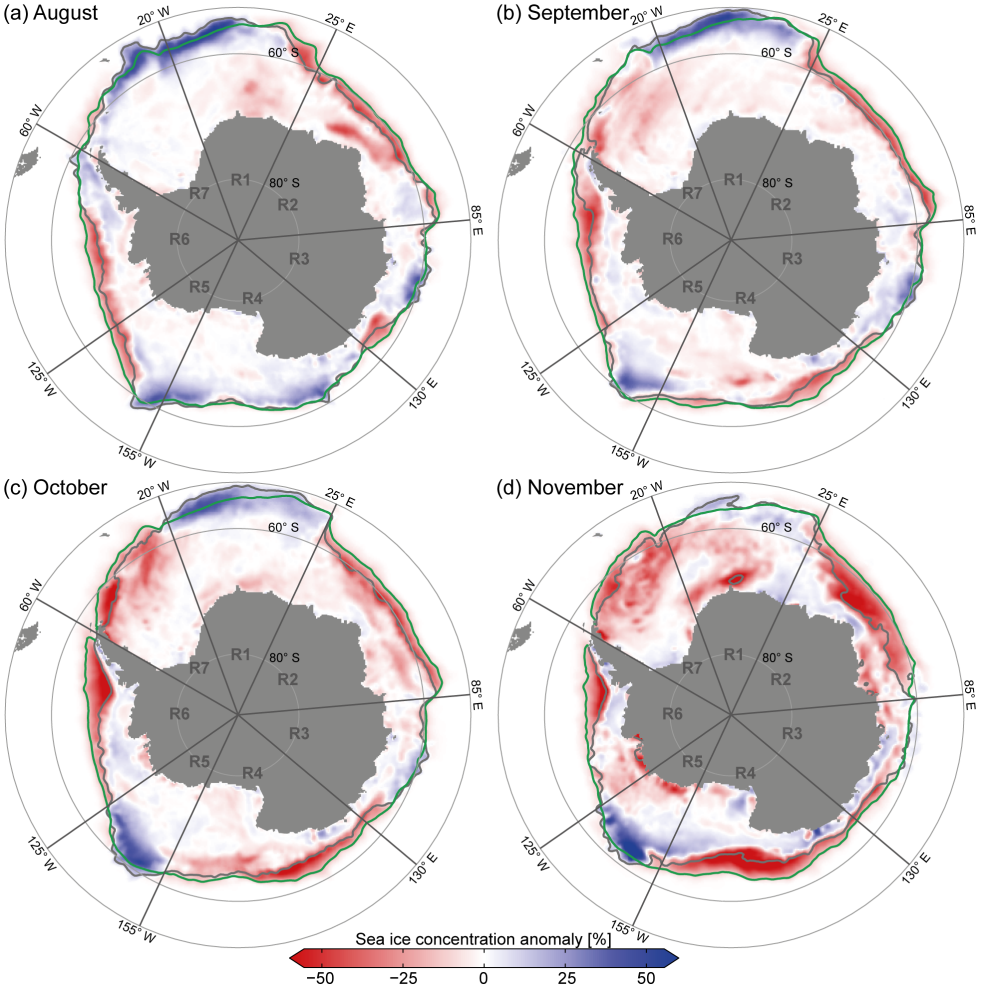

Fig. 3

The Cryosphere Discuss., https://doi.org/10.5194/tc-2017-192
Manuscript under review for journal The Cryosphere
Discussion started: 22 September 2017
© Author(s) 2017. CC BY 4.0 License.

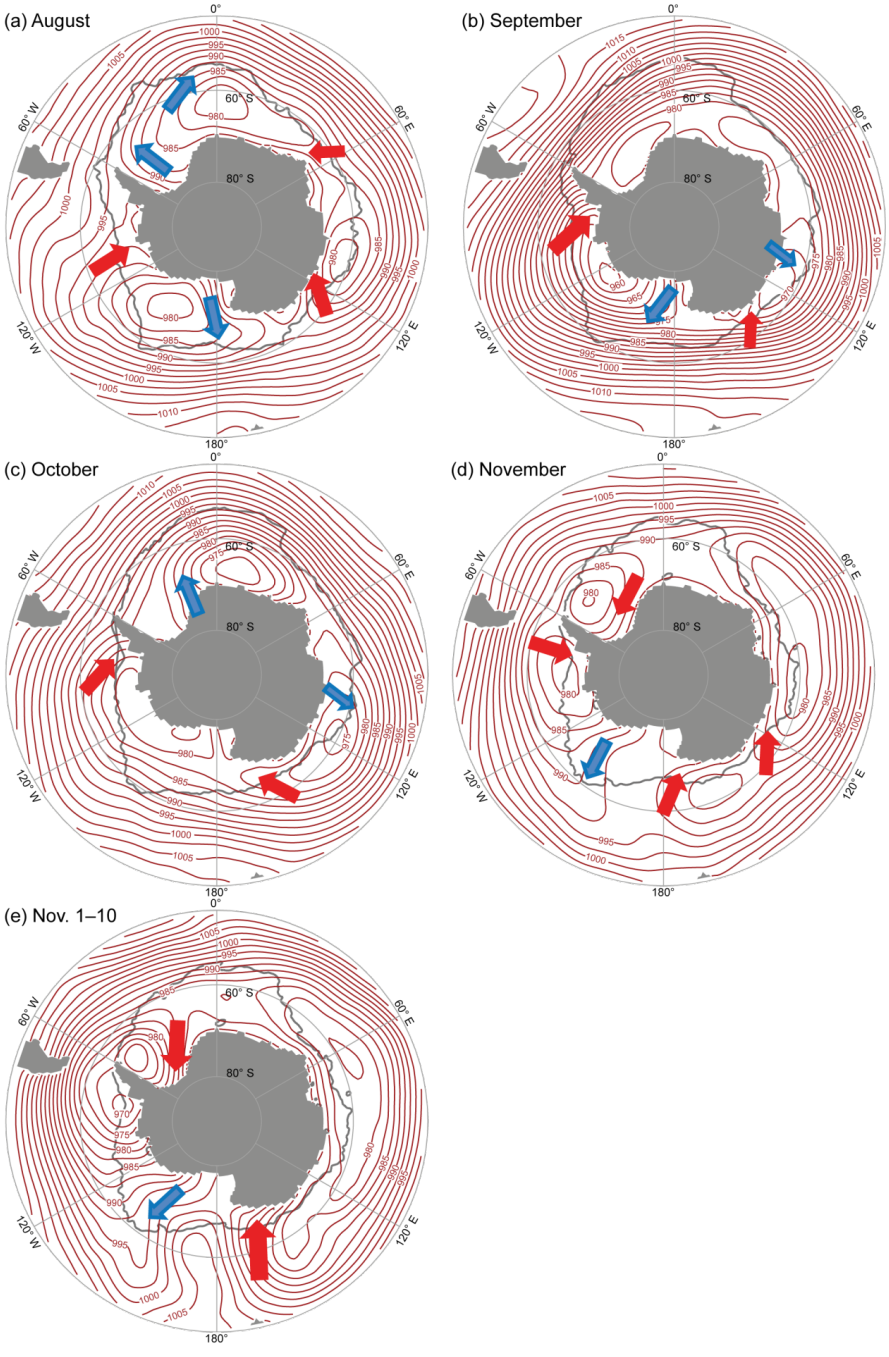

Fig. 4

The Cryosphere Discuss., https://doi.org/10.5194/tc-2017-192
Manuscript under review for journal The Cryosphere
Discussion started: 22 September 2017
© Author(s) 2017. CC BY 4.0 License.

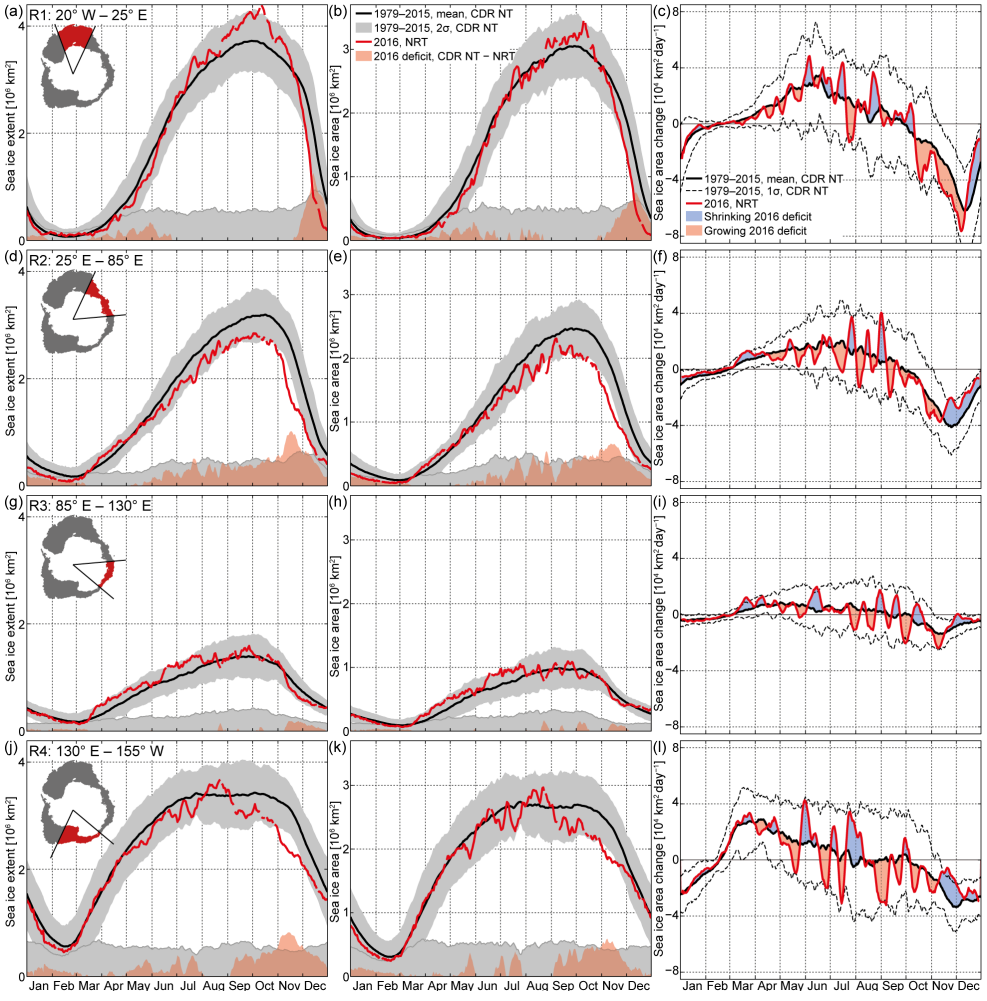

The Cryosphere Discuss., https://doi.org/10.5194/tc-2017-192
Manuscript under review for journal The Cryosphere
Discussion started: 22 September 2017
© Author(s) 2017. CC BY 4.0 License.

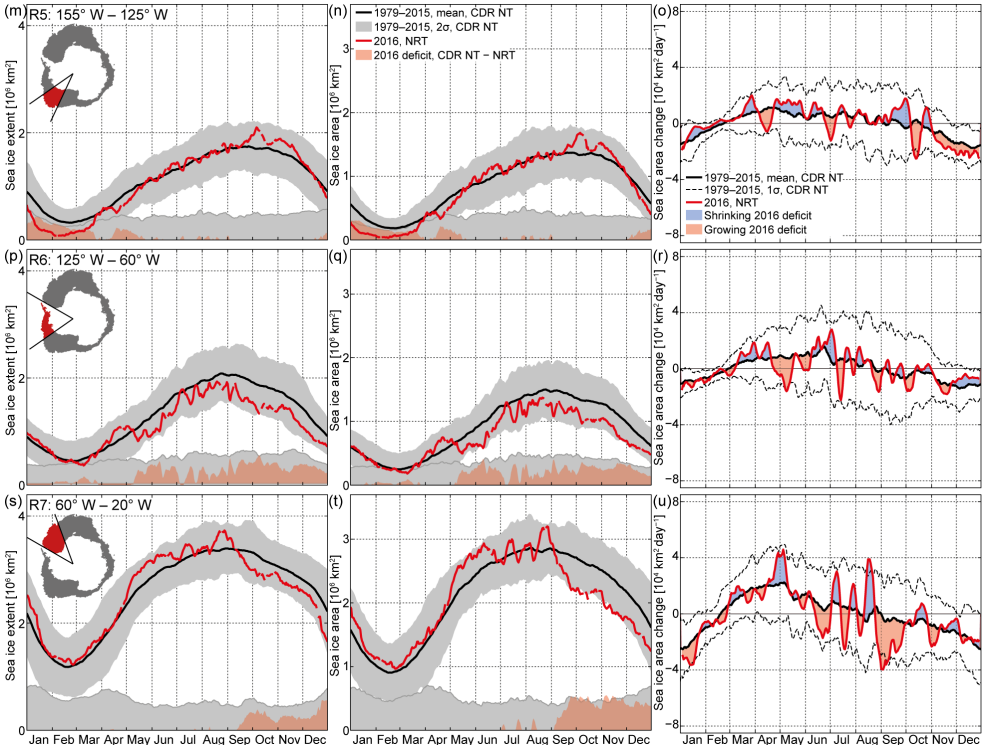

Fig. 5

The Cryosphere Discuss., https://doi.org/10.5194/tc-2017-192
Manuscript under review for journal The Cryosphere
Discussion started: 22 September 2017
© Author(s) 2017. CC BY 4.0 License.

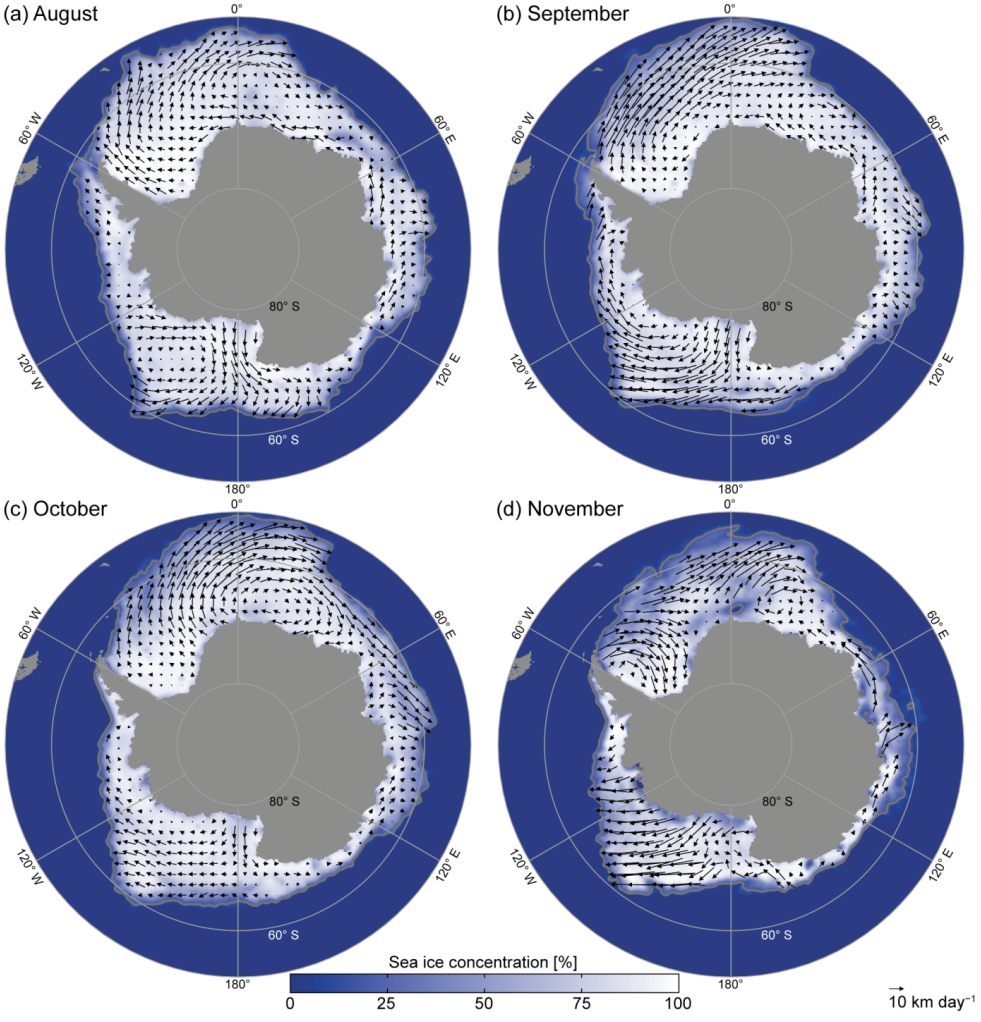

Fig. 6

The Cryosphere Discuss., https://doi.org/10.5194/tc-2017-192
Manuscript under review for journal The Cryosphere
Discussion started: 22 September 2017
© Author(s) 2017. CC BY 4.0 License.

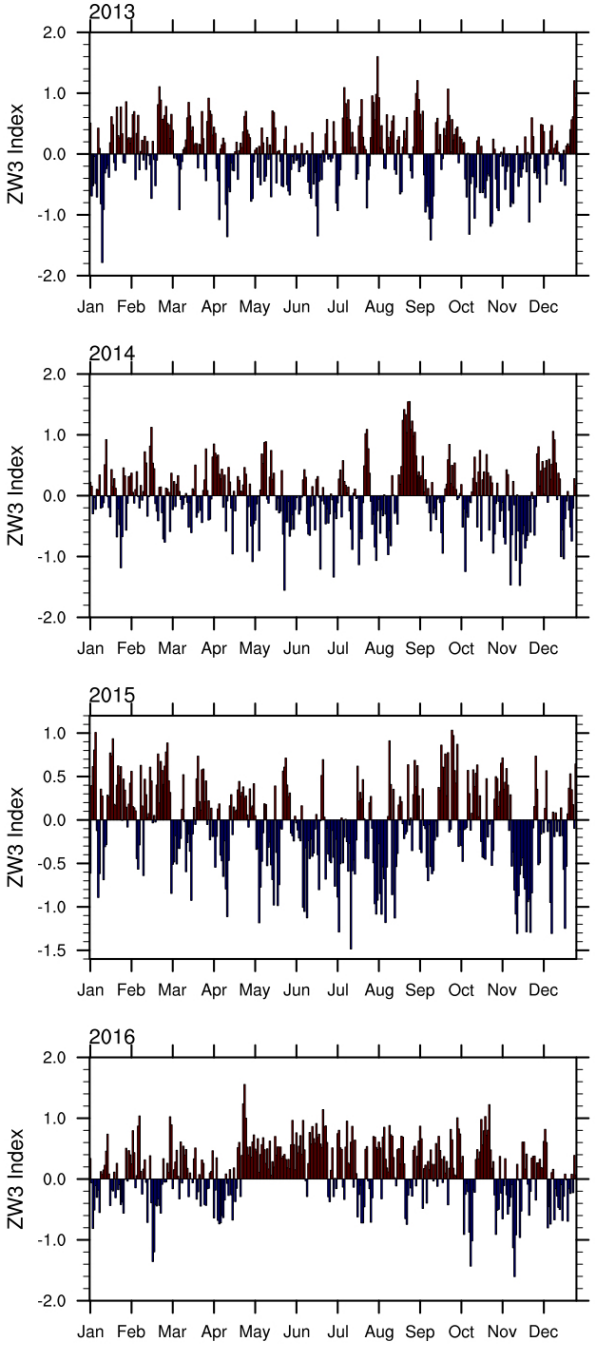

Fig.7a

The Cryosphere Discuss., https://doi.org/10.5194/tc-2017-192
Manuscript under review for journal The Cryosphere
Discussion started: 22 September 2017
© Author(s) 2017. CC BY 4.0 License.

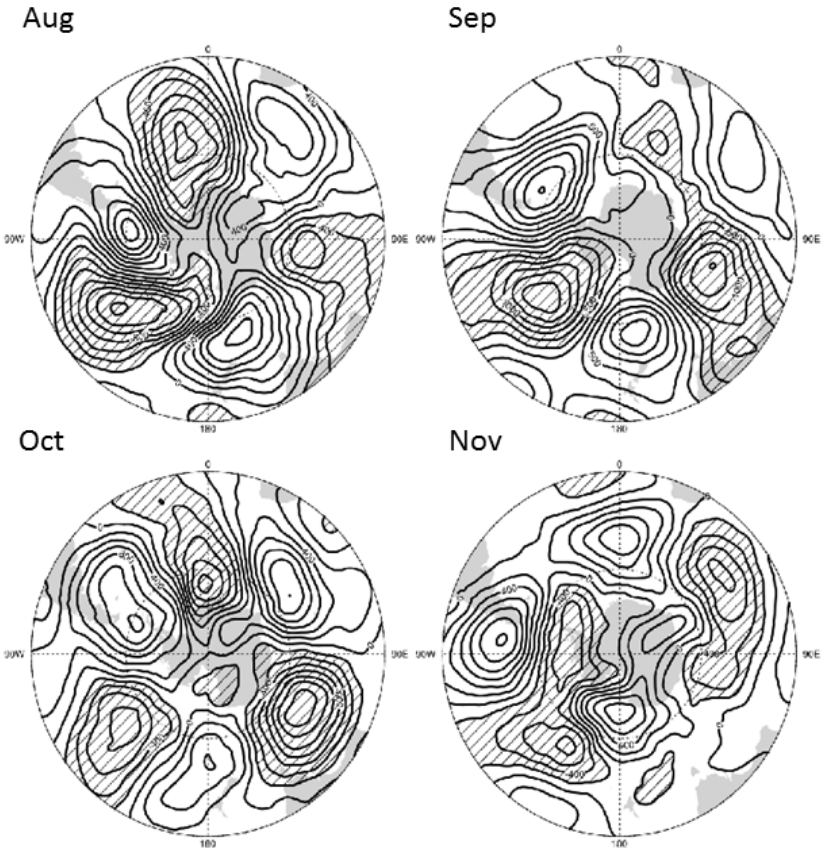

Fig. 7b

The Cryosphere Discuss., https://doi.org/10.5194/tc-2017-192
Manuscript under review for journal The Cryosphere
Discussion started: 22 September 2017
© Author(s) 2017. CC BY 4.0 License.

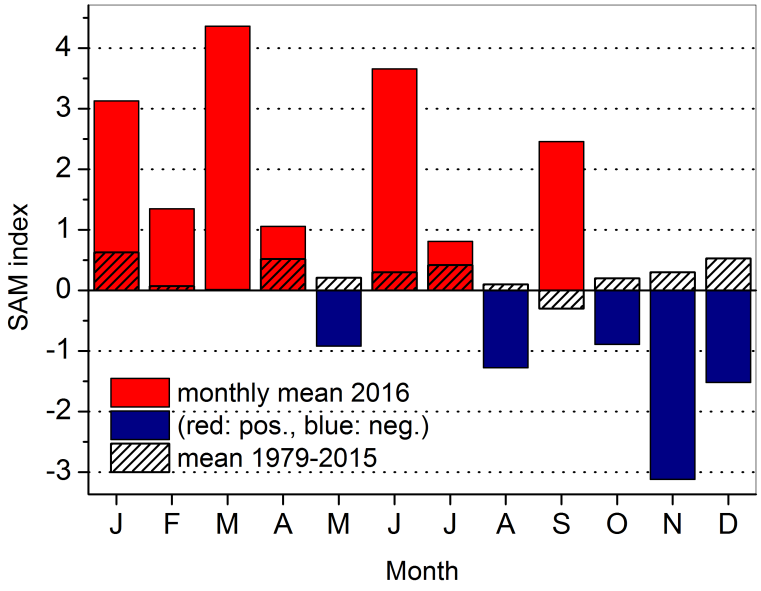

Fig. 8